Synthesis and electronic spectra of novel merocyanine dyes bearing a maleimide ring incorporated into the methine chains

Yasuhiro Shigemitsu[a,*], Manabu Sugimoto[b], Sachiko Itonaga[c],
Kaori Komiya[c], Yoshinori Tominaga[c]

[a]*Industrial Technology Center of Nagasaki, 2-1303-8, Ikeda, Omura, Nagasaki 856-0026, Japan*
[b]*Department of Applied Chemistry and Biochemistry, Faculty of Engineering, Kumamoto University,
Kurokami, Kumamoto 860-8555, Japan*
[c]*Center for Instrumental Analysis, Nagasaki University, 1-14, Bunkyo-machi, Nagasaki 852-8521, Japan*

Abstract

The present article describes the synthesis of new polymethine dyes with a heterocyclic ring incorporated into the methine chain. 1-Alkyl-2 or 4-methylpyridinium salts and related compounds **1a–e** reacted at the exocyclic double bond with cyano- or methoxycarbonyl heterocycles bearing a methylthio group **2a–d** to give new polymethine dyes **3a–n** in good yield. This reaction occurred by an addition-elimination mechanism, involving nucleophilic attack of cyclic enamines at carbon deficient atoms on the heterocycles followed by elimination of methylmercaptan. The polymethine dyes obtained are red, violet, and blue in color with the absorption peaks at 524–614 nm. Semi-empirical as well as ab-initio quantum chemical calculations were used to theoretically characterize their $\pi-\pi^*$ absorption maxima in the visible region which plays a decisive role in their color appearances.
© 2002 Elsevier Science Ltd. All rights reserved.

Keywords: Merocyanine dyes; Maleimides; Electronic spectra; Molecular orbital calculations

1. Introduction

Ketene dithioacetals are important and useful reagents for the synthesis of a variety of heterocycles which have one more methylthio group on the heterocyclic ring. These heterocycles can be used as useful intermediates for the synthesis of new heterocycles such as fused pyridines, pyrimidines, pyrones, etc. [1]. In addition to the vast amount of merocyanine dyes already synthesized [2], the present paper describes the prepararion of new merocyanine dyes with a pyrrole ring as heterocycle incorporated into the methane chains where the methylthio group serves as a leaving group [3]. Merocyanine dyes with two extreme (zwitterionic and non reso-nant) electronic structures have attracted much

---

* Corresponding author. Tel.: +81-957-52-1133; fax: +81-957-52-133.
*E-mail address:* shige@tc.nagasaki.go.jp (Y. Shigemitsu).

attention from the theoretical viewpoint and various quantum chemical calculations have been carried out to obtain information on their quantitative color prediction [4]. In this paper a series of semi-empirical and ab-initio quantum chemical calculations are presented to provide theoretical insights into the spectral properties of the species.

2. Synthesis and electronic spectra

Novel maleimides, 4-methylthio-1H-pyrrole-2,5-diones bearing cyano or methoxycarbonyl group as electron withdrawing group are important and versatile synthetic starting materials [5] and also are effective for the construction of merocyanine dyes. These heterocycles are generally obtained by the reaction of ketene dithioacetals with nitromethane in the presence of potassium carbonate in good yield. Methylene bases prepared from the corresponding quaternary salts are nucleophilic reagents that paralleled the Brooker derivatives of the basic heterocycles. The reaction of 1,2-dimethylpyridinium iodide **1a** with 4-cyano-1-methyl-3-methylthio-1H-pyrrole-2,5-dione **2a** in the presence of potassium carbonate as a base in dimethyl sulfoxide at room temperature gave a red violet product, **3a**, in 47% yield. As shown in Fig. 1, **1a** also smoothly reacted with **2b** bearing a methyl ester group to give the corresponding polymethine dye **3b** in 39% yield. Reaction of 1-ethylquinolinium iodide **1b** with **2a** under the same reaction conditions gave the corresponding methine dye **3c** in 81% yield. The other polymethine dyes **3d–h** were also readily obtained via the reaction of the corresponding quaternary salts **1b, 1c** with **2a–d**. The reaction of 1,4-dimethylpyridinium iodide **1d** and 4-methyl-1-isoamyl quinolinium iodide **1e** with **2a** and **2b** gave the corresponding polymethine dyes **3i–n** (Fig. 2) whose first intense low energy absorption maxima ranged from 524–614 nm in the visible region (Table 1). Among **3a–n**, **3m** possessed an absorption peak in the long wavelength region which would be promising for medical use such as chromogenic reagents in clinical diagnosis [6].

3. Computational details

Molecular mechanics and semi-empirical MO calculations were performed using CaChe software [7] and ab-initio calculations were made using GAUSSIAN98 software [8]. As preliminary geometry exploration, the molecular mechanics program CONFLEX [9] was employed to find the most stable and second stable conformers for **3a–n** in order to judge which conformer was energetically favored in both cis and trans states with respect to the two central bonds connecting the two moieties. The first and second stable conformers then served as starting structures for the full geometry optimization, with AM1 method [10] to determine the minimum energy structures. These were refined further by density functional theory (DFT) with Dunning's correlation-consistent polarized valence double-zeta(cc-pVDZ) [11] basis set in conjunction with the combined Becke three-parameter hybrid exchange/Lee-Yang-Parr correlation functional (B3LYP) [12], using default convergence criterion on force and displacement. On AM1-optimized geometries for **3a–n**, spectral calculations using the semi-empirical ZINDO method [13] were carried out with INDO/S preset parameters to obtain the $\pi-\pi^*$ lowest transition energies along with their associated oscillator strengths. The default SECI (Single Excited Configuration Interaction) method distributes 28 electrons among the highest 14 occupied MOs and the lowest unoccupied 14 MOs designed to generate the single exited configurations, denoted as SECI(28,28) hereafter. To study the size dependency of the CI space on the excitation energies, the extended SECI (44,44) for **3a** were acomplished to give its absorption peak at 543 nm and SECI(28,28) at 534 nm. This finding allowed us to employ the medium-size SECI(28,28) caclulation for the remaining dyes. A series of ab-initio spectral caclulations (CIS [14], RPA [15] and TD-DFT [16]) were used on the optimized geometries in terms of DFT(B3LYP)/cc-pVDZ aforementioned. Solvent effects were considerd using IPCM method [17] combined with RPA/4-31G and PCM method [18] with DFT(B3LYP)/6-31+G*, respectively.
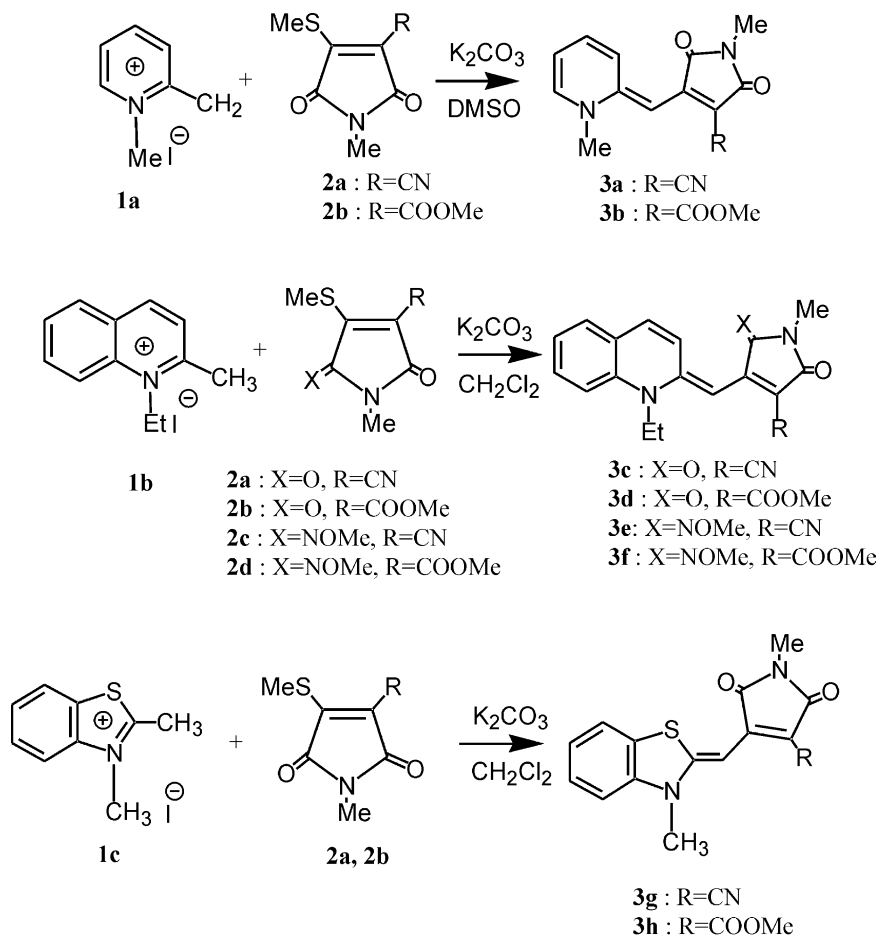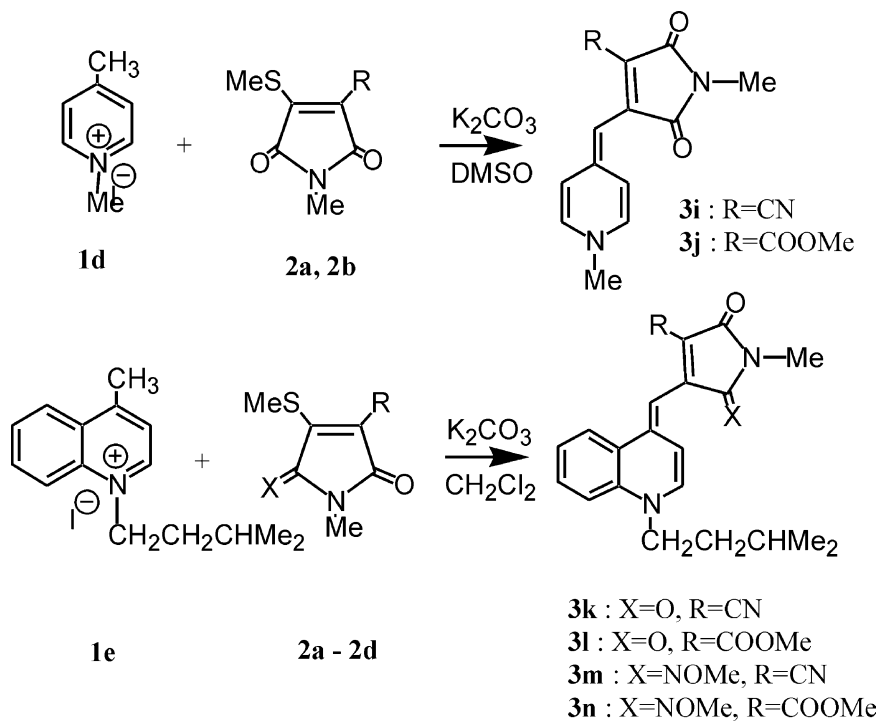
Fig. 1. Synthetic scheme of **3a–h**.

4. Results and discussion

Regarding theoretical geometries, Table 2 shows that AM1 predicted substantially distorted conformers around the two central bonds for dyes **3a–n** regardless of the presence of intra-steric hindrances. In contrast, the DFT calculation, which is generally considered to be more reliable than AM1 in geometry explorations, gave more planar structures for the molecules excluding **3e**, **3f**, **3m** and **3n** with appreciably intra-steric hindrances between the-NOMe group on the maleimide ring and the hydrogen on the counterpart moiety illustrated in Table 3. For **3g** and **3h**, the existence of nonbonded sulfur-oxygen intramolecular interaction, which has been reported for small molecules

as well as for biological systems [19], were indicated because the planar structures were restored even if the optimizations were begun from the somewhat distorted forms. As for electronic spectra, the following experimental characteristics surface and are assessed in terms of theoretical results hereafter;

1. The first intense low energy absorption maxima of **3i–n** showed bathochromic shifts compared with the corresponding **3a–f** with the same substituents (Table 1). For instance, **3i** exhibited its absorption peak at 545nm by 21nm bathochromic shift from that of **3a**. This is attributed to the elongation of the π-conjugated backbone of **3i–n** rather than **3a–h**.

Fig. 2. Synthetic scheme of **3i–n**.

Table 1
UV spectral data (theoretical and experimental) of **3a–n**

	Solution color	ZINDO(AM 1[a]/DFT[b])		TDDFT (vacuum/in EtOH[c])		Experiment	
		λ_{max} (nm)	Oscillator strength	λ_{max} (nm)	Oscillator strength	λ_{max} (nm)	log ε
3a	Wine red	546/502	0.41/0.84	479/479	0.43/0.43	524	4.32
3b	Wine red	537/497	0.56/0.65	465/456	0.32/0.37	535	4.46
3c	Blue	519/466	0.56/0.87	459/465	0.56/0.59	574	4.69
3d	Blue	537/492	0.60/1.18	487/494	0.65/0.64	563	4.55
3e	Blue	509/483	0.44/0.93	492/500	0.51/0.52	578	4.75
3f	Blue	554/479	0.19/0.89	490/508	0.45/0.45	566	4.86
3g	Purple	468/463	0.42/0.80	472/482	0.52/0.56	542	4.59
3h	Purple	446/433	0.29/0.79	442/457	0.59/0.59	546	4.73
3l	Purple	522/478	0.66/0.95	461/480	0.55/0.52	545	4.51
3j	Wine red	550/494	0.47/1.09	473/475	0.57/0.53	534	4.47
3k	Blue	544/512	0.38/0.71	553/572	0.41/0.42	604	4.77
3l	Blue	590/506	0.29/0.66	550/581	0.38/0.39	595	4.62
3m	Blue	503/493	0.43/0.53	516/539	0.36/0.38	614	4.92
3n	Blue violet	511/473	0.30/0.47	512/552	0.32/0.32	587	4.61

[a] Geometries optimized with AM1.
[b] Geometries optimized with B3LYP/cc-pVDZ.
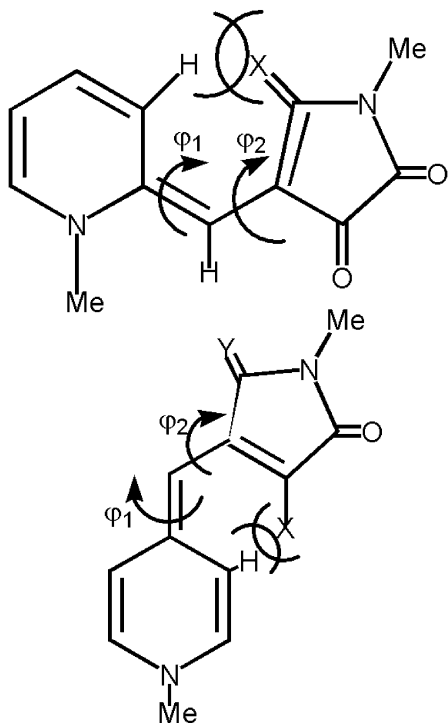[c] Solvent effects considered with PCM option.

Table 2
The heat of formation (HF) and key torsional angles (φ_1, φ_2) of the AM1-optimized first and second stable conformers

	Most stable conformer			Second stable conformer		
	HF (kcal/mole)	φ_1	φ_2	HF (kcal/mole)	φ_1	φ_2
3a	55.3	154	19	57.1	178	44
3b	−57.9	171	134	−55.6	169	46
3c	65.8	169	42	67.0	176	48
3d	−46.1	172	135	−42.2	176	56
3e	114.8	168	49	120.0	177	99
3f	8.9	177	112	9.6	176	90
3g	66.4	170	38	66.6	176	136
3h	−38.3	178	56	−34.2	166	71
3i	52.9	5	148	53.4	170	138
3j	−56.9	11	43	−49.0	11	47
3k	47.4	7	49	49.0	3	130
3l	−60.6	6	53	−50.3	7	133
3m	93.2	9	46	102.0	3	128
3n	−18.3	4	124	−2.8	6	125

2. Different subsystems deriving from the corresponding quaternary salts substantially affected the extent of the red shift, i.e., in the order of pyridine < benzothiazole < quinoline for **3a–h** and pyridine < quinoline for **3i–n**, respectively.

3. The introduction of electron donating/withdrawing substituents (methoxycarbonyl/cyano group) on the 4-methyl-thiomaleimide ring gave the opposite peak shift depending on the corresponding pairs. (These shifts would be too small (ca. 10nm) for the calculations to reproduce correctly.) In the cases of (**3c**,**3d**), (**3e**,**3f**), (**3i**,**3j**), (**3k**,**3l**) and (**3m**,**3n**), where the cyano-substituted dye shows a hypsochromic shift relative to the dye with methoxycarbonyl group whereas for (**3a**,**3b**) and (**3g**,**3h**) the cyano dye exhibited a bathochromic shift relative to the methoxycarbonyl dye.

Table 3
Two key tortional angles for **3a–n** equilibrium structures optimized with B3LYP/cc-pVDZ

	φ_1	φ_2
3a	180.3	180.5
3b	166.9	159.4
3c	169.7	169.2
3d	175.4	4.3
3e	173.6	25.0
3f	169.3	36.2
3g	180.0	0.7
3h	180.4	−0.4
3i	0.1	0.6
3j	0.2	−0.6
3k	0.4	−0.1
3l	4.2	3.9
3m	14.6	156.2
3n	14.8	148.8

4. Intra-steric hindrances between two bridged parts that would force **3e, 3f, 3m** and **3n** to be twisted do not cause the significant absorption peak shift (less than 10 nm) compared with other molecules.

ZINDO calculations on AM1-optimized geometries unfortunately predicted neither the correct absorption peak position nor the systematic deviations from the observed absorption peaks. For instance, the calculated λ_{max} for **3a** was overevaluated by 22 nm from the observed λ_{max} while that for **3m** was underevaluated by 113nm. Concerning the effect of the ring system on t spectral peaks, the bathochromic shift in the order of pyridine < benzothiazole < quinoline for **3a–h** and pyridine < quinoline for **3i–n** were not well reproduced. Bathochromic shifts of **3i–n** compared with the corresponding **3a–n** was not predicted correctly either. The situation remained unchanged even if DFT-optimized geometries were adopted where the theoretical peaks moved considerably to the shorter wavelength region relative to AM1-optimized ones. These poor performances would be due to the methodological limitation of the ZINDO method with the default parameters. The lowest excited state of **3a** was mainly describable with the HOMO-LUMO $\pi-\pi^*$ single electron excitation with the dominantly large CI coefficient (0.969). Moving onto a series of ab-initio calculations, Table 4 demonstrates

that the CIS and RPA theoretical peaks of **3a**, as is well known, were substantially underestimated [16,20] by over 100 nm, i.e., 171nm for CIS/4-31G and 146 nm for RPA/4-31G respectively, with slight (ca. 10 nm) improvement in considering of the solvent effect with the IPCM method for RPA/4-31G. With TD-DFT(B3LYP)/4-31G, the absolute deviation was considerably improved to 71 nm. Encouraged by this preliminary calculation on **3a**, we adopted TD-DFT using more extensive set 6-31 + G* in order to obtain a good compromise between computational cost and qualitative accuracy for the remaining molecules **3b–n**. The predicted maxima were underevaluated by 56–115 nm in vacuum as shown in Table 1. Despite considerable gaps between predicted peak positions and experimental ones, systematic deviations between them could be obtained in contrast to the ZINDO results. The two major bathochromic shifts, one derived from the ring system in the order of pyridine < benzothiazole < quinoline for **3a–h** and pyridine < quinoline for **3i–n**, and another from the elongation of π-conjugation were both reproduced qualitatively with some exceptions. For instance the absorption peak of **3c** was underevaluated compared to that of **3a**. Taking into account solvent effect with the PCM option, prediction were improved to a 14–109 nm. In particular, the PCM calculation gave a considerable red shift with more than 20 nm for **3i–n** with less than 20 nm for **3a–h** (inversely 9 nm blue-shift for

Table 4
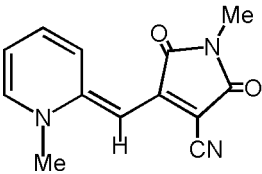Ab-initio calculations for $\pi-\pi^*$ absorption peak of **3a** (in parentheses: IPCM option for EtOH)

	CIS	RPA	TD-DFT (B3LYP)	
	4-31G	4-31G	4-31G	6-31G**
λ_{max} (nm)	362	389 (396)	470	468
Oscillator strength	0.99	0.78 (0.72)	0.40	0.41

Table 5
Physical data for compounds **3a**–**n**

Entry	Yield (%)	Mp (°C) (Recryst, Solv)	Formula	Analysis (%) Calcd. (found)			Infrared frequencies ν (cm^{-1}) in KBr	Electron ionization mass spectrometer data m/z (relative intensity)	^{1}H-NMR δ (ppm)
				C	H	N			
3a[a]	47	276–279 (MeOH)	$C_{13}H_{11}N_3O_2$ (241.252)	64.72 (64.76	4.60 4.70	17.42 17.31)	2195 (CN), 1722 (C=O), 1622 (C=O), 1585, 1422, 1118	242 (M + +1, 17), 241 (M +, 100), 156 (59), 155 (70), 78 (26), 44 (30)	289 (3H, s, Nme), 4.09 (3H, s, Nme), 6.34 (1H, s, =CH), 7.41 (1H, dd, J = 7.8, 6.6 Hz, 5-H), 7.77 (1H, d, J = 8.4 Hz, 3-H), 8.20 (1H, dd, J = 8.4, 7.8 Hz, 4-H), 8.62 (1H, d, J = 6.6 Hz, 6-H)
3b[a]	39	256–258 (MeOH)	$C_{14}H_{14}N_2O_4$ (274.279)	61.31 (61.10	5.14 5.12	10.21 10.05)	1705 (C=O), 1665 (C=O), 1635, 1550, 1525, 1438, 1365, 1140	274 (M +, 43), 243 (20), 216 (21), 158 (14), 131 (16), 44 (100)	2.84 (3H, s, Nme), 3.57 (3H, s, Ome), 4.03 (3H, s, Nme), 6.30 (1H, s, =CH), 7.06 (1H, d, J = 6.6 Hz, 3-H), 8.13 (1H, d, J = 6.7 Hz, 6-H), 8.23–8.28 (2H, m, 4, 5-H)
3c[b]	81	294–296 (MeOH)	$C_{18}H_{15}N_3O_2$ (305.34)	70.81 (71.06	4.95 5.07	13.76 13.67)	2795 (CN), 1735 (C=O), 1675 (C=O), 1545, 1430, 1142, 1120	306 (M + +1, 21), 305 (M +, 100), 304 (25), 220 (27), 192 (24), 143 (66), 44 (43)	1.67 (3H, t, J = 7.1 Hz, CH$_2$–CH$_3$), 3.09 (3H, s, Me), 4.57 (2H, J = 7.1 Hz, CH$_2$–CH$_3$), 6.17 (1H, s, =CH), 7.55 (1H, m, 6-H), 7.71–7.86 (4H, m, 3, 5, 6, 7, 8-H), 8.11 (1-H, d, J = 9.2 Hz, 4-H)
3d[b]	66	120–122 (MeOH)	$C_{19}H_{18}N_2O_4$ (338.366)	67.45 (66.60	5.36 5.36	8.28 8.12)	1710 (C=O), 1675 (C=O), 1650 (C=O), 1525, 1430, 1140, 1120	339 (M + +1, 21), 338 (M +, 82), 307 (17), 280 (31), 279 (100), 278 (10), 253 (14), 222 (11), 195 (15), 194 (31), 193 (13), 143 (31), 44 (86)	1.68 (3H, t, J = 7.1 Hz, CH$_2$–CH$_3$), 3.07 (3H, s, Me), 3.80 (3H, s, Ome), 4.60 (2H, q, J = 7.2 Hz, CH$_2$–CH$_3$), 6.65 (1H, bs, =CH), 7.51 (1H, m, 6-H), 7.68–7.83 (5H, m, 3, 4, 5, 7, 8-H)
3be	94	210–212 (MeOH and Toluene)	$C_{19}H_{18}N_2O_4$ (334.381)	68.25 (68.34	5.43 5.46	16.76 16.68)	2180 (CN), 1718 (C=O), 1522, 1430, 1375, 1440	335 (M + +1, 24), 334 (M +, 100), 319 (8), 303 (8), 275 (8), 256 (8), 246 (16), 219 (10), 191 (14), 167 (15), 143 (37), 128 (11), 69 (27), 57 (25), 44 (96)	1.57 (3H, t, J = 7.1 Hz, CH$_2$–CH$_3$), 3.18 (3H, s, Nme), 3.98 (3H, s, Ome), 4.36 (2H, q, J = 7.1 Hz, CH$_2$–CH$_3$), 5.87 (1H, s, =CH), 7.36 (1H, m, 6-H), 7.44 (1H, d, J = 9.3 Hz, 3-H), 7.50 (1H, d, J = 8.5 Hz, 8-H), 7.61–7.68 (2H, m, 5, 7-H), 7.74 (1H, d, J = 9.3 Hz, 4-H)
3f[b]	98	137–139 (MeOH)	$C_{20}H_{21}N_3O_4$ (367.408)	65.38 (65.44	5.76 5.80	11.44 11.57)	2950, 170 (C=O), 1680, 1545, 1435, 1215, 1040	368 (M + +1, 25), 367 (M +, 100), 308 (28), 143 (23), 69 (24), 57 (20), 44 (25), 43 (21)	1.51 (3H, t, J = 7.2 Hz, CH$_2$–CH$_3$), 3.36 (3H, s, Nme), 3.80 (3H, s, Ome), 3.99 (3H, s, Ome), 5.98 (1H, s, =CH), 7.13–7.18 (2H, m, 3, 6-H), 7.26–7.30 (2H, m, 4, 8-H), 7.45 (1H, d, J = 7.3 Hz, 5-H), 7.48 (1H, m, 7-H)

Table 5 (*continued*)

Entry	Yield (%)	Mp (°C) (Recryst, Solv)	Formula	Analysis (%) Calcd. (found)			Infrared frequencies ν (cm^{-1}) in KBr	Electron ionization mass spectrometer data m/z (relative intensity)	^{1}H-NMR δ (ppm)
				C	H	N			
3g[a]	92	329–330 (MeOH and toluene)	$C_{15}H_{11}N_3O_2S$ (297.334)	60.59 3.73 14.14 3.81 (S) (60.14 3.81 13.88 10.65 (S))			2180 (CN), 1725 (C=O), 1660 (C=O), 1140, 980, 770	298 (M + +1, 19), 297 (M +, 100), 212 (17), 148 (22), 75 (17), 44 (84), 43 (19)	2.96 (3H, s, Nme), 3.98 (3H, s, Nme), 6.34 (1H, s, =CH), 7.44 (1H, m, aromatic-H), 7.62 (1H, m, aromatic-H), 7.85 (1H, m, aromatic-H), 8.12 (1H, m, aromatic-H)
3h[b]	88	315–318 (MeOH and toluene)	$C_{16}H_{14}N_3O_4S$ (330.361)	58.14 4.27 8.48 9.70 (S) (58.18 4.27 8.48 9.58 (S))			1724 (C=O), 1682 (C=O), 1645, 1540,1300, 1150	331 (M + +1, 20), 330 (M +, 100),299 (33), 271 (32), 187 (14), 186 (22), 44 (33)	3.09 (3H, s, Nme), 3.89 (3H, s, Ome), 7.38 (1H, m, 7-H), 7.39 (1H, s, =CH), 7.54 (1H, m, 5-H), 7.70 (1H, d, J=7.7 Hz, 4-H), 7.75 (1H, m, 6-H)
3i[b]	92	313–315 (MeOH)	$C_{13}H_{11}N_3O_2$ (241.249)	64.72 4.60 17.42 (64.46 4.70 17.21)			2196 (CN), 1725 (C=O), 1675 (C=O), 1560, 1432, 1140	242 (M + +1, 16), 241 (M +, 100), 156 (37), 107 (10), 79 (17), 78 (18), 69 (11), 57 (15), 55 (14), 44 (45), 43 (19)	2.82 (3H, s, Nme), 4.05 (3H, s, Nme), 6.20 (1H, s, =CH), 7.73 (2H, d, J=7.2 Hz, 3, 5-H), 8.39 (2H, d, J=6.4 Hz, 2, 6-H)
3j[b]	80	263–265 (MeOH)	$C_{14}H_{14}N_2O_4$ (274.276)	61.31 5.14 10.21 (61.02 5.13 10.17)			1710 (C=O), 1665 (C=O), 1632, 1550, 1440, 1370, 1140	275 (M + +1, 5), 274 (M +, 27), 243 (10), 216 (7), 44 (100), 43 (14)	2.83 (3H, s, Nme), 3.58 (3H, s, OMe), 4.00 (3H, s, Nme), 6.29 (1H, s, s=CH), 7.05 (1H, d, J=6.2 Hz, 5-H), 8.13 (1H, d, J=6.8 Hz, 3-H), 8.28–8.22 (2H, m, 2, 6-H)
3k[b]	97	235–237 (MeOH)	$C_{21}H_{21}N_3O_2$ (347.420)	72.60 6.09 12.10 (72.58 6.12 11.99)			2950, 2175 (CN), 1730 (C=O), 1670 (C=O), 1540, 1430, 1380, 1225	348 (M + +1, 10), 347 (M +, 100), 192 (11), 44 (14), 43 (63)	1.07 (6H, d, J=6.0 Hz, CH (CH$_3$)2), 1.79 (1H, m, CH (CH$_3$)2), 1.83 (2H, m, C-CH$_2$-C), 3.08 (3H, s, Nme), 4.40 (2H, t, J=7.7 Hz, N-CH$_2$), 6.91 (1H, s, =CH), 7.58 (1H, bs, 3-H), 7.63 (1H, ddd, J=8.5, 7.5, 1.0 Hz, 6-H), 7.68 (1H, d, J=8.5 Hz, 8-H), 7.84 (1H, ddd, J=8.5, 7.5, 1.0 Hz, 7-H), 8.03 (1H, d, J=7.0 Hz, 2-H), 8.42 (1H, dd, J=8.5, 1.0 Hz, 5-H)
3l[b]	87	204–206 (MeOH)	$C_{22}H_{24}N_2O_4$ (380.437)	69.46 6.36 7.36 (69.30 6.41 7.37)			1730 (C=O), 1685 (C=O), 1650, 1530, 1430, 1380, 1225, 1160	381 (M + +1, 18), 380 (M +, 66), 349 (10), 322 (14), 45 (14), 44 (100), 43 (24), 41 (16)	1.04 (6H, d, J=5.5 Hz, CH (CH$_3$)2, 1.79–1.84 (3H, m, CH$_2$CH$_2$CH (CH$_3$)2), 3.07 (3H, s, Nme), 3.84 (3H, s, OMe), 4.35 (2H, t, J=6.9 Hz, N-CH$_2$), 7.35 (1H, bs, 3-H), 7.55–7.60 (3H, m, =CH, 5, 8-H), 7.72 (1H, d, J=7.6 Hz, 2-H), 7.76 (1H, m, 7-H), 8.45 (1H, d, J=8.5 Hz, 5-H)

Table 5 (*continued*)

Entry	Yield (%)	Mp (°C) (Recryst, Solv)	Formula	Analysis (%) Calcd. (found)			Infrared frequencies ν (cm⁻¹) in KBr	Electron ionization mass spectrometer data *m/z* (relative intensity)	¹H-NMR δ (ppm)
				C	H	N			
3m[b]	86	203–205 (MeOH)	$C_{22}H_{24}N_4O_2$ (376.462)	70.79 (70.24	6.43 6.49	14.88 14.92)	2970, 2930, 2195 (CN), 1695 (C=O), 1615, 1525, 1510, 1385, 1225	377 (M + +1, 27), 376 (M + , 100), 69 (35), 57 (30), 55 (30), 44 (91), 43 (39), 41 (32)	1.03 (6H, d, *J* = 6.1 Hz, CH (CH₃)2), 1.75–1.80 (3H, m, CH₂, CH), 3.19 (3H, s, Nme), 3.99 (3H, s, OMe), 4.19 (2H, t, *J* = 1.8 Hz, N-CH₂), 6.72 (1H, s, =CH), 7.05 (1H, d, *J* = 7.0 Hz, 3-H), 7.46 (1H, m, 6-H), 7.41 (1H, d, *J* = 7.9 Hz, 8-H), 7.52 (1H, d, *J* = 7.9 Hz, 8-H), 7.66 (1H, m, 7-H), 8.29 (1H, d, *J* = 8.7 Hz, 5-H)
3n[b]	86	158–160 (MeOH)	$C_{23}H_{27}N_3O_4$ (409.489)	67.46 (67.30	6.65 6.60	10.28 10.28)	2900, 1710 (C=O), 1620, 1520, 1440, 1382, 1230	410 (M + +1, 29), 409 (M + , 100), 158 (25), 143 (27), 57 (31), 44 (91), 43 (32)	1.00 (6H, d, *J* = 6.0 Hz, CH (CH₃)2), 1.56–1.72 (3H, m, CH₂, CH), 3.16 (3H, s, Nme), 3.84 (3H, s, OMe), 3.90 (3H, s, OMe), 3.98 (3H, s, OMe), 3.98 (2H, m, N–CH₂) 6.31 (1h, s, =CH, 6.75 (d, *J* = 7.5 Hz, 3-H), 6.83 (d, *J* = 7.8 Hz, 2-H), 7.16–7.54 (3H, m, 6-H, 7-H, 8-H), 8.03 (1H, *J* = 7.8 Hz, 5-H)

[a] In DMSO-d_6.
[b] In CDCl₃.

3b), indicating that the solute-solvent interactions stabilize the excited sates of **3i–n** than **3a–h**. Summarizing our discussions on the π−π* absorption peaks of **3a–n**, the ZINDO predictions were untrustworthy and TD-DFT, which has been found suitable for many cases [21], was not adequate either from the viewpoint of absolute coincidences between the experimental and the theoretical absorption peaks even when taking solvent effects into consideration. It was however satisfactory in providing qualitatively correct systematic correlations with the experiments, indicating its usefulness for molecular design of the further derivatives. We would need to check the performance of other exchange correlation functionals [22] of TD-DFT in aiming to further improvement of the quantitative prediction in future.

5. Experimental

All melting points were determined in a capillary tube and are uncollected. Infrared spectra were recorded using potassium bromide pellets employing a JASCO S10 spectrometer. Uultraviolet (uv) absorption spectra were determined in 100% ethanol on a Shimazu UV3100pc spectrometer. Nuclear magnetic resonance (nmr) spectra were obtained on Gemini 300NMR (300 NHz) and JEOL-GX-400 (400 MHz) spectrometers with tetramethylsilane as internal standard. Mass (ms) spectra were recorded on a JEOL MA-DX303 mass spectrometer. Elemental analyses were performed at the Microanalytical Laboratory of the Center for Instrumental Analysis in Nagasaki University. All physical data (yield, melting point, elemental analysis, IR, mass and ^{1}H-NMR) are summarized in Table 5.

5.1. 2-(4-Cyano-1-methyl-2,5-dioxo-1H-pyrrol-3-yl)methylene-1-methyl-1,2-dihydropyridine (3a)

5.1.1. Method A
A mixture of **1a** (1.17 g, 5 mmol), **2a** (0.91 g, 5 mmol), potassium carbonate (1.38 g, 10 mmol), and 20 ml of dimethyl sulfoxide were stirred at room temperature for 3 h, during whicht time it changed from yellow to red, and then dark violet.

The reaction mixture was poured into 200 ml of water and was allowed to stand for 3 h. The precipitate that appeared was collected by filtration. The product was recrystallized from methanol after air drying to give dark red leaflets (0.57 g, 2.37 mmol).

5.1.2. Method B
A mixture of **1a** (1.17 g, 5 mmol), **2a** (0.91 g, 5 mmol), potassium carbonate(1.38 g, 10 mmol), and 30 ml of dichhloromethane were stirred at room temperature for 12 h, during which time it changed from yellow to red, and then dark violet. After reaction, insoluble material such as excess potassium carbonate was removed by filtration and the resulting dark violet mixture was filtered through filter paper. After the insoluble material was washed with about 30 ml of acetone and 100 ml of dichloromethane, the filtrate was transferred to a separating funnel and washed successively 100 ml of water. The combined organic layer was dried over magnesium sulfate and evaporated on a rotary evaporator, leaving a dark red residue which was crystallized from methanol to give red leaflets (0.73 g, 3.03 mmol) of **3a**. uv(ethanol) λ_{max} nm(log ϵ): 255(4.04), 287(3.78), 524(4.32).

5.2. 2-(4-Methoxycarbonyl-1-methyl-2,5-dioxo-1H-pyrrol-3-yl)methylene-1-methyl-1,2-dihydropyridine (3b)

5.2.1. Method A
This compound (1.23 g, 4.4 mmol) was synthesized from **1a** (1.25 g, 5mmol), **2b** (1.07 g, 5 mmol) in a manner similar to that described for the preparation of **3a**. An analytical sample was recrystallized from methanol to give greenish black crystals; uv(ethanol) λ_{max} nm(log ε): 265(4.29), 307.5(4.08), 535(4.46).

5.3. 2-(4-Cyano-1-methyl-2,5-dioxo-1H-pyrrol-3-yl)methylene-1,2-dihydro-1-ethylquinoline (3c)

5.3.1. Method A
This compound (1.36 g, 4.45 mmol) was synthesised from **1b** (1.50 g, 5 mmol), **2a** (1.17 g, 5 mmol) in a manner similar to that described for the preparation of **3a**. An analytical sample was

recrystallized from methanol to give greenish black crystals; uv(ethanol) $\lambda_{\max}$ nm(log ε): 237(4.12), 283(3.52), 289(3.52), 329(3.54), 574(4.27).

5.4. 1-Ethyl-2-(4-methoxycarbonyl-1-methyl-2,5-dioxo-1H-pyrrol-3-yl)methylene-1,2-dihydroquinoline (3d)

5.4.1. Method A

This compound (0.78 g, 2.31 mmol) was synthesized from **1b** (1.50 g, 5 mmol), **2b** (1.07 g, 5 mmol) in a manner similar to that described for the preparation of **3a**. An analytical sample was recrystallized from methanol to give dark greenish crystals; uv(ethanol) $\lambda_{\max}$ nm(log ε): 265(4.29), 308(4.08), 535(4.46).

5.5. 2-(4-Cyano-5-methoxyimino-1-methyl-2-oxo-1H-pyrrol-3-yl)methylene-1,2-dihydroquinoline (3e)

5.5.1. Method A

This compound (0.656 g, 1.79 mmo) was synthesized from **1b** (0.60 g, 2 mmol) and **2c** (0.49 g, 2.0 mmol) in a manner similar to that described for the preparation of **3a**. An analytical sample was recrystallized from a mixture of methanol and toluene to give greenish prisms; uv(ethanol) $\lambda_{\max}$ nm(log ε): 238(4.39), 333(3.79), 365(3.65), 578(4.75).

5.6. 2-(4-Methoxycarbonyl-5-methoxyamino-1-methyl-2-oxo-1H-pyrrol-3-yl)methylene-1,2-dihydroquinoline (3f)

5.6.1. Method A

This compound (0.656 g, 1.79 mmo) was synthesized from **1b** (0.60 g, 2.0 mmol) and **2d** (0.49 g, 2.0 mmol) in a manner similar to that described for the preparation of **3a**. An analytical sample was recrystallized from methanol to give black needles; uv(ethanol) $\lambda_{\max}$ nm(log ε): 246(4.61), 263(4.59), 325(4.14), 552(4.86), 566(4.86).

5.7. 2-(4-Cyano-1-methyl-2,5-dioxo-1H-pyrrol-3-yl)methylene-2,3-dihydro-3-methylbenzothiazole (3g)

5.7.1. Method A

This compound (1.37 g, 4.61 mmol) was synthesized from **1c** (1.45 g, 5.0 mmol) and **2a** (1.17 g, 5.0 mmol) in a manner similar to that described for the preparation of **3a**. An analytical sample was recrystallized from a mixture methanol and toluene to give black violet needles; uv(ethanol) $\lambda_{\max}$ nm(log ε): 523, 291, 239;

5.8. 2-(4-Methoxycarbonyl-1-methyl-2,5-dioxo-1H-pyrrol-3-yl)methylene-3-methyl-2,3-dihydrobenzothiazole (3h)

5.8.1. Method A

This compound (0.58 g, 1.76 mmo) was synthesized from **1c** (0.58 g, 2.0 mmol) and **2b** (0.43 g, 2.0 mmol) in a manner similar to that described for the preparation of **3a**. An analytical sample was recrystallized from a mixture of methanol and toluene to give black needles; uv(ethanol) $\lambda_{\max}$ nm(log ε): 220(4.31), 248(4.17), 303(4.29), 546(4.73).

5.9. 4-(4-Cyano-1-methyl-2,5-dioxo-1H-pyrrol-3-yl)methylene-1-methyl-1,4-dihydropyridine (3i)

5.9.1. Method A

This compound (0.62 g, 2.57 mmol) was synthesized from **1d** (1.17 g, 50 mmol) and **2a** (0.91 g, 5.0 mmol) in a manner similar to that described for the preparation of **3a**. An anlytical sample was recrystallized from methanol to give greenish black crystals; uv(ethanol) $\lambda_{\max}$ nm(log ε): 245(4.13), 303(3.96), 545(4.51); ms.

5.10. 4-(4-Methoxycarbonyl-1-methyl-2,5-dioxo-1H-pyrrol-3-yl)methylene-1-methyl-1,4-dihydropyridine (3j)

5.10.1. Method B

This compound (1.15 g, 4.18 mmol) was synthesized from **1d** (1.17 g, 5.0 mmol) and **2b** (1.0 g, 5.0 mmol) in a manner similar to that described for the preparation of **3a**. An analytical sample was recrystallized from methanol to give greenish black crystals; uv(ethanol) $\lambda_{\max}$ nm(log ε): 266(4.19), 308(4.08), 534(4.47).

5.11. 1-Isoamyl-4-(4-Cyano-1-methyl-2,5-dioxo-1H-pyrrol-3-yl)methylene-1-methyl-1,4-dihydroquinoline (3k)

5.11.1. Method A

This compound (0.75 g, 1.84 mmol) was synthesized from **1e** (0.68 g, 2.0 mmol) and **2a** (0.36 g, 2.0 mmol) in a manner similar to that described for the preparation of **3a**. An analytical sample was recrystallized from methanl to give greenish black leaflets; uv(ethanol) λ_{max} nm(log ε): 244(4.34), 283(3.89), 308(4.02), 603(4.71).

5.12. 1-Isoamyl-4-(4-methoxycarbonyl-1-methyl-2,5-dioxo-1H-pyrrol-3-yl)methylene-1,4-dihydroquinoline (3l)

5.12.1. Method A

This compound (0.83 g, 2.2 mmol) was synthesized from **1e** (0.68 g, 2.0 mmol) and **2b** (0.43 g, 2.0 mmol) in a similar manner to that described for the preparation of **3a**. An analytical sample was recrystallized from methanol to give greenish black leaflets; uv (ethanol) λ_{max} nm(log ε): 595(4.62), 306(4.04), 243(4.35).

5.13. 4-(4-Cyano-5-methoxyamino-1-methyl-2-oxo-1H-pyrrol-3-yl)methylene-1-isoamyl-1,4-dihydroquinoline (3m)

5.13.1. Method A

This compound (0.65 g, 1.73 mmol) was synthesized from **1e** (0.68 g, 2.0 mmol) and **2c** (0.42 g, 2.0 mmol) in a manner similar to that described for the preparation of **3a** . An analytical sample was recrystallized from methanol to give dark violet leaflets; uv(ethanol) λ_{max} nm(log ε): 248(4.35), 308(3.90), 344(3.91), 614(4.92).

5.14. 1-Isoamyl-1,4-dihydro-4-(5-methoxyimino-4-methoxycarbonyl-1-methyl-2-oxo-1H-pyrrol-3-yl)methylenequinoline (3n)

5.14.1. Method A

This compound (1.25 g, 3.65 mmol) was synthesized from **1e** (0.68 g, 2.0 mmol) and **2d** (0.49 g,

2.0 mmol) in a manner similar to that described for the preparation of **3a**. An analytical sample was recrystallized from methanol to give dark violet needles; uv(ethanol) λ_{max} nm(log ε): 205(4.65), 244(4.28), 270(4.17), 341(3.88), 587(4.61).

References

[1] (a) Tominaga Y. Trend in Heterocyclic Chemistry 1991; 2:43;
(b) Dieter RK. Tetrahedron 1986;42:3029.

[2] (a) Gommper R, Hagele W. Chem Ber 1966;99:2885;
(b) Edwards HD, Kendall JD. Chem Abst 1951;45:2804 U.S. 2533233, 1950;
(c) Mizuyama K, Tominaga Y, Matsuda Y, Kobayashi G. Yakugaku Zasshi 1975;95:290–8;
(d) Venkataraman K. The Chemistry of Synthetic Dyes 1952;2:1143, ibid **4**, 212 (1971).

[3] (a) Ila H, Junjappa H, Mohanta PK. In: Gribble GW, Gilchrist T, editors. Progress in heterocyclic chemistry. New York: Pergamon; 2001. p. 1–24
(b) Junjappa H, Ila H, Asokan CW. Tetrahedron 1990; 46:5423;
(c) Dieter RK. Tetrahedron 1986;42:3029;
(d) Kolbe M. Synthesis 1990;171.

[4] (a) Peters AT, Freeman HS. Colour chemistry: the design and synthesis of organic dyes and pigments, advances in colour chemistry series. New York: Elsvier Applied Science; 1991;
(b) Waring DR, Hallas G, editors. The chemistry and application of dyes. New York: Plenum Press, 1991;
(c) Sturmer DM. Chem Heterocycl Comp 1977;30:441;
(d) Fabian J, Nakazumi H, Matsuoka M. Chem Rev 1992; 92:1197;
(e) Griffiths J. Colour and constitution of organic molecules. London: Academic Press; 1976;
(f) Fabian J, Hartmann H. Light absorption of organic colorants. Berlin: Springer-Verlag; 1980.

[5] (a) Tominaga Y, Yoshioka N, Kataoka S. Heterocycles 1996;43:1597;
(b) Tominaga Y, Yoshioka N, Minematsu H, Kataoka S. Heterocycle 1996;44:85;
(c) Tominaga Y, Ushirogouchi A, Matsuda Y, Kobayashi G. Chem Pharm Bull 1984;32:3384.

[6] Tominaga Y, Itonaga S, Kouno T, Shigemitsu Y. Heterocycles 2001;55(8):1447.

[7] Cache work system ver. 4.1 (Cache Scientific Inc.).

[8] Frisch MJ, Trucks GW, Schlegel HB, Scuseria GE, Robb MA, Cheeseman JR. Gaussian 98 (Revision A.10). Pittsburgh PA: Gaussian; 1998.

[9] Goto H, Osawa E. CONFLEX 3.

[10] Dewar JS, Zoebisch EG, Hearly EG, Stewart JJP. J AmChemSoc 1985;107:3902.

[11] Dunning Jr TH. J Chem Phys 1989;90:1007.

[12] (a) Becke AD. J Chem Phys 1993;98:5648;
(b) Lee C, Yang W, Parr RG. Phys Rev B 1988;37:785.

[13] Ridley J, Zener MC. Theoret Chim Acta (Berl) 1973;32:111.

[14] Foresman JB, Head-Gordon M, Pople JA, Frish MJ. J Phys Chem 1992;96:135.

[15] Joergensen P, Simons J. Second quantization-based methods in quantum chemistry. New York: Academic Press; 1981.

[16] (a) Bauernshmitt R, Ahlrichs R. Chem Phys Lett 1996; 256:454;
(b) Casida ME, Jamorski C, Casida KC, Salahub DR. J Chem Phys 1998;108:4439;
(c) Startmann RE, Scuseria GE, Frish MJ. J Chem Phys 1998;109:8218.

[17] Foresman JB, Keith TA, Wiberg KB, Snoonian J, Frish MJ. J Phys Chem 1996;100:16098.

[18] Barone V, Cossi M. J Phys Chem 1998;A102:1995 and references therein.

[19] (a) Burling FT, Goldstein BM. J Am Chem Soc 1992; 114:2313;
(b) Nagao Y, Hirata T, et al. J Am Chem Soc 1998; 120:3104;
(c) Wu S, Greer A. J Org Chem 2000;65:4883;
(d) Iwaoka M, Tomoda S, et al. Chem Lett 2001;132.

[20] Hirata S, Gordon M-H. Chem Phys Lett 1999; 302:375.

[21] (a) Fabian J, Mamn M, Petiau M. J Mol Mod 2000; 6:177;
(b) Petiau M, Fabian J. J Mol Struct (THEOCHEM) 2001;538:253.

[22] Tozer DJ, Amos RD, Handy NC, Roos BO, Serrano-Andres L. Mol Phys 1999;97(7):859.